033549-1-F

Micromachined Antennas for Microwave and MM-Wave Applications

FINAL REPORT
ONR Contract: N00014-95-1-1299

Linda P.B. Katehi

April 1998

33549-1-F = RL-2463

Final Report

on

Micromachined Antennas for Microwave and mm--Wave Applications

by

Linda P.B. Katehi

The University of Michigan

ONR Parent Contract: N00014-95-1-0546
ONR AASERT Contract: N00014-95-1-1299

April 1998

Reporting Period:

Progress Report: January 1997-April 1998

Final Technical Report: August 15, 1995-April 30, 1998

Graduate Student:

John Papapolymerou (student)

Faculty:

Prof. Linda P.B. Katehi and Prof. Gabriel Rebeiz

Other Contributing Research Staff:

Jong-Gwan Yook

Manuscripts Published or Submitted During the Reporting Period:

1. L.P.B. Katehi, et. al., Industrial Electronics Handbook, Chapter on "Si Micromachining in High-Frequency Applications," pp. 1547-1575, CRC Press, 1997.
2. J. Papapolymerou, J. East and L.P.B. Katehi, "GaAs vs. Quartz FGC Lines for MMIC Applications," in Press IEEE Transactions on Microwave Theory and Techniques.
3. J. Papapolymerou, J. East, L.P.B. Katehi, M. Kim and I. Mehdi, "Millimeter-Wave GaAs Monolithic Multipliers," to be presented in the 1998 International Symposium on Microwave Theory and Techniques, Baltimore, MD, June 1998.
4. J. Papapolymerou, J. East and L.P.B. Katehi, "W-Band Monolithic Multipliers," Proceedings of the 1997 International Symposium on Microwave Theory and Techniques, pp. 1225-1228, Denver, CO, June 1997.
5. J.G. Yook and L.P.B. Katehi, "Suppression of Surface Waves Using Micromachining Techniques," to be presented in the 1998 International Symposium on Microwave Theory and Techniques, Atlanta, GA, June 1998.

Honors and Awards

- 1997 Best Paper Award by the International Microelectronics and Packaging Society (IMAPS)
- First Prize in Symposium Paper Award Contest with Katherine Herrick for the paper ÒW-Band Micromachined Finite Ground Coplanar (FGC) Line Circuit Elements," IEEE MTT-S, Denver, CO, June 1997

Brief Description of Performed Research

This AASERT project concentrates on the development of high-efficiency Si-Based and GaAs-Based lines, multipliers and micromachined antennas. The effort in this project is to combine high-efficiency and Si-based packaging techniques to develop fully integrated mixer/multiplier pairs that are also integrated with a high-efficiency antenna to provide a complete receiver chip. This project so far has been split into three parts: (a) High-Performance FGC lines printed on Si, Quartz or GaAs substrates, (b) High-Efficiency Mixer/Multiplier Pairs and (c) Micromachined High-Efficiency Antennas.

Each one of these subjects has been addressed separately and has almost been completed. As the last effort in the student's dissertation all of these three components will be combined to provide the W-Band monolithic high-efficiency receiver discussed above. In the following we will discuss the progress of this work during the last year of this AASERT award separately. Since Finite Ground Coplanar lines (FGC) have provided the baseline technology for the W-band multiplier we will combine the discussion on these two subjects in Part I while micromachined antennas will be discussed in Part II separately.

PART I: (a) High-Efficiency FGC Lines and W-Band Monolithic FGC Multipliers

The main objective of this effort was to design and fabricate W and D band monolithic multipliers with high efficiency and broad bandwidth on GaAs, by using the Finite Ground Coplanar (FGC) line as the guiding structure. Before proceeding with the design of the multipliers, the performance of the FGC line was experimentally investigated. Several FGC lines with different characteristic impedances were fabricated and tested on GaAs and the results were compared with those of lines with the same geometrical characteristics on low loss quartz substrate. In addition, the effect of passivation was addressed by covering the GaAs FGC lines with a thin film of polyimide. Measurements showed the following:

The effective dielectric constant of all of the lines that were tested was nearly constant for a frequency range of 2 to 118 GHz. This indicates the propagation of a nearly pure TEM mode that allows to analyze and design high frequency FGC based MMIC's with ideal transmission line theory. The effective dielectric constant of the FGC lines on GaAs covered with a 2 μm and a 3 μm thick polyimide increased slightly by 1.4% and 2.8% respectively, when compared with the bare FGC lines, indicating that the addition of the polyimide does not change significantly the propagation characteristics of the FGC line. The attenuation per physical length (dB/cm) was highest for the 3 μm polyimide line on GaAs and smallest for the line on quartz. The increase though that is caused with the addition of polyimide is small (12% for the 2 μm and 23% for the 3 μm in W-band) when compared with the bare FGC line on GaAs, and as a result the total loss in actual circuits covered with polyimide for passivation will not increase substantially.

The attenuation per guided wavelength (dB/λ_g) is the same for all the lines tested and has a $1/\sqrt{f}$ dependence versus frequency, indicating that the loss is mainly ohmic and independent of the substrate material and thickness for a given line geometry. The

attenuation per guided wavelength decreases as the impedance of the FGC line increases in a non-linear way. Since it was found that in terms of loss GaAs with or without polyimide and quartz are equivalent for the same FGC geometry, the choice of material for a substrate depends on other design criteria. If low cost is a major issue then quartz can be chosen with the active devices being flip-chip bonded to it. On the other hand if the active devices must be monolithically integrated with the rest of the circuitry, then GaAs is more appropriate with a thin overlay of polyimide for passivation. GaAs is also more suitable for applications above 120 GHz, such as the D-band multipliers, where the flip-chip bonding process increases fabrication complexity considerably.

Having analyzed the FGC line, we proceeded with the design and fabrication of W and D band monolithic multipliers with FGC lines. In contrast with waveguide multipliers where the mounting structure is designed around the varactor geometry, in the monolithic multiplier the diode and the circuit were designed together. A computer program was developed where the input design parameters are the epitaxial layer doping and thickness, the desired real diode impedance, the quality factor Q of the diode and the input frequency and power. The output data from this program are the embedding impedance of the diode at the second harmonic, the required diode area and the estimated reverse bias voltage. Based on the results of this program W band multipliers were designed with quality factors of 2 and 3 and diode areas of 74 and 65 μm^2 ,respectively. The D band multipliers had a Q of 2 and a diode area of 40 μm^2. The epitaxial layer had a doping of 10^{17} /cm^3 and a thickness of 4000 A, while the real part of the impedance for all diodes was 50 Ohms. The matching and isolation networks on the input and output side were designed using FGC lines with the information regarding attenuation and effective permittivity based on the experimental results that were performed first. Stubs were used on the input side of the circuit to trap the second harmonic output and on the output side to trap the fundamental frequency.

Measurements indicated a 17.6% peak efficiency at 76 GHz with a 3 dB bandwidth of 8 GHz and an output power of 66 mW for the multiplier with Q=2, while the Q=3 multiplier had a 22.9% peak efficiency and a bandwidth of 6 GHz at 70 GHz. The latter

combination of efficiency and bandwidth makes this multiplier design unique since it offers both a very good efficiency and a broad bandwidth. The experimental results were in accordance with the simulation predictions that indicated that the low Q circuits would have wider bandwidths and lower efficiencies than the higher Q versions. For the D band multipliers an uncalibrated efficiency of 1% and output power of 100 μW was measured at 160 GHz with a 3 dB bandwidth of 5 GHz. These results can be attributed to the fact that the doping level was not optimum for the D band circuits (only for the W band) and that substrate moding was occurring at 160 GHz due to the geometry of the line. Improvement of the D band multiplier can be achieved by optimizing the epitaxial layer profile (i.e. increase the doping) and decreasing the width of the ground strips of the FGC lines.

As a conclusion we could say that FGC based monolithic multipliers have exhibited a very good efficiency in conjunction with a broad bandwidth and that their design can be easily scaled from lower to higher frequencies without losing the excellent characteristics.

PART II: Micromachined Antennas

Microstrip antennas are used in a broad range of applications from communication systems (radars, telemetry and navigation) to biomedical systems, primarily due to their simplicity, conformability and low manufacturing cost. With the recent development of microwave and millimeter-wave integrated circuits and the trend to incorporate all microwave devices on a single chip for low-cost and high density, there is a need to fabricate microstrip antennas in a monolithic fashion with the rest of the circuitry on semiconducting materials such as Silicon, GaAs or InP. These antennas despite their planar character and low cost suffer from high surface-wave excitation resulting in compromised efficiency, reduced bandwidth and degradation of the radiation pattern. Furthermore, in monolithic designs the feed lines share in most cases the same interface with the antennas and lead into parasitic radiation which deforms the antenna pattern and increases cross-talk. The most recent work on micromachined antennas is on the understanding of efficiency, bandwidth and coupling and their comparison to conventional antennas. This work will be completed at the end of April and will be submitted for publication to the Transactions of Antennas and Propagation

APPENDIX A: Published /Submitted Papers

W Band Monolithic Multipliers

Fred Brauchler*, John Papapolymerou, Jack East and Linda Katehi
Electrical Engineering and Computer Science Department
The University of Michigan
Ann Arbor, Michigan

Abstract

This paper describes the realization of a W band planar monolithic multiplier using finite ground coplanar lines. These lines provide near TEM low loss propagation to W band and enhance multiplier performance. The developed MMIC multipliers have demonstrated 93 mW output power, 26% efficiency and output bandwidth from 70 to 80 GHz.

Introduction

Local oscillator sources are an important part of all high frequency receiver applications. These sources have a long experimental history mostly based on Schottky barrier diodes. Early diodes were honeycomb anode chips with a whisker contact and were characterized by very small parasitics. However, they were difficult to handle, have problems with thermal cycling and vibrations and have performance that is critically dependent on the shape of the whisker. Even with these problems, whisker contacted multipliers were the most common millimeter and submillimeter wave sources until the late 1980s. In 1987 Bishop et. al. proposed the microchannel structure as an alternative high frequency planar diode [1]. This structure was much easier to handle and mount in waveguide blocks. Furthermore, the structure could also be used to fabricate multiple diodes for the same mount. An example of this type of device is given by Rizzi et.al. [2] with the multiplier having a peak output of 55 mW at 174 GHz, and an efficiency of 25% with an output of 37 mW using a balanced combination of two diode pairs.

Presently most millimeter wave multipliers are of waveguide type. Waveguide circuits have the lowest loss and highest Q needed for efficient multiplier operation. Furthemore, they can include tuners and backshorts needed to optimize for peak performance. However, waveguide mounts are complex to design and fabricate, and become more difficult and expensive to machine with increasing frequency and smaller size. MMIC multipliers have many advantages compared to waveguide structures. They can provide low cost and small size circuits, while large numbers can be fabricated at the same time using integrated circuit fabrication techniques. However, planar multipliers have some limitations. They exhibit higher loss and lower Q than the waveguide ones. It is also much more difficult to include tuning elements. Even with these limitations, some very useful MMIC multipliers have been reported. Chen et. al. [3] described a planar MMIC multiplier with an output power of 65 milliwatts and an efficiency of 25% at 94 GHz using a microstrip circuit.

Microstrip and coplanar waveguides are two guiding structures that are used extensively for high frequency MMIC applications. One problem associated with the microstrip approach is that line characteristics depend on the substrate thickness and moding can occur at high frequencies unless the substrate is thinned. CPW has a performance which is less dependent on the substrate thickness, but problems can occur because of parasitic parallel plate waveguide modes which can only be suppressed by use of via holes. However, the via holes make circuit fabrication more difficult and can cause additional problems if placed incorrectly. The more complex propagation properties add to circuit design problems since complicated line models are needed to correctly predict results.

This paper describes circuits fabricated by use of a modified coplanar waveguide structure with finite width ground planes. This Finite Ground Coplanar (FGC) line overcomes many of the problems associated with conventional CPW and microstrip line, and can be scaled easily to higher frequencies. The narrow ground planes reduce the effect of parallel plate modes thus eliminating the need for via holes. Wafer thinning is not required and the back side metallization does not

*Currently at Texas Instruments Research Laboratory.

0-7803-3814-6/97/$5.00 © IEEE

affect line characteristics. The line geometry is chosen so that the width of the entire structure is less than half the dielectric wavelength at the highest frequency under consideration. The loss normalized to wavelength has an inverse square root dependence indicating an ohmic nature. The loss is approximately 0.25 dB/mm at 100 GHz. The measured data was fitted to a lossy TEM transmission line model using LIBRA. There is a close fit between the measured and modeled results, again indicating that FGC line can be correctly described by a non-dispersive lossy TEM line. A detailed description of these lines is given by Brauchler[3].

Design of FGC Multipliers

The FGC line elements are used as a starting point for the multiplier design. Experimental measurements gave a range of 20 to 80 Ω for line impedances. A nonlinear multiple reflection program was used to design the multiplier [4]. In a conventional multiplier design, the varactor diode is usually specified and the multiplier is designed around it. Here, the diode parameters become part of the design process. The operating frequency sets the doping level, and the peak RF voltage swing, limited by the breakdown voltage, sets the active epitaxial layer width. The multiplier bias point is also a parameter. Multiplier operation varies from a resistive mode, where the input Q at the pump frequency is in the range from 1 to 2 and the efficiency is modest, to a reactive mode where the input Q and the efficiency are both higher. The realized impedance for high Q as compared to the design impedance is more sensitive to small changes in element values than similar low Q topologies. Waveguide multipliers can be designed for higher Q, with modest differences in the designed vs. realized impedances, adjusted with tuners and backshorts. Similar impedances in an MMIC multiplier are fixed, with the bias point being the only available "tuning". The multiple reflection code was modified to adjust the diode area and bias so that the required embedding impedances could be realized with FGC lines and the input Q was approximately two.

Results and Discussions

A variety of multipliers including series and shunt diodes and single and multiple diodes were designed, fabricated and tested. The best results, which have been obtained with the diode pair shunt structure, will be described here. A photograph of the multiplier is shown in Figure 1 with a close up view of the diodes shown in Figure 2. It is designed with 50 Ω input and outputs on the ends, a second harmonic trap on the input side and a fundamental trap on the output sides. The varactor diodes are connected to the signal line with inductive lines. The multiplier is evaluated using on wafer probing at the input and output ports. The input and output measurements are calibrated to the tips of the probes using Ka band and W band HP 8510 test sets and with power meters at the pump and output frequencies. A Ka band TWT is used as the source. This combination of input and output test set frequencies limited the output frequency range to 70 to 80 GHz. The measured output power and efficiency of the multiplier is shown in Figure 3. The first design iteration provided a multiplier with peak efficiency equal to 16.3 % and peak output power equal to 72 mW at 80 GHz. The design worked well over the entire measurement frequency range. The efficiency and return loss from 70 to 80 GHz for a constant 100 mW input power are shown in Figure 4. The -3 dB efficiency bandwidth is wider than the 10 GHz measurement bandwidth. A second iteration of this multiplier provided an output power of 93 mW. The design efficiency of this multiplier was 32%. The estimated loss of the input and output circuits based on line measurements was 1.1 dB and the return loss at the peak efficiency point was -7.5 dB. The resulting multiplier internal efficiency is 26%, in reasonable agreement with the model prediction. This output power level is among the best reported for MMIC multipliers at W band.

Acknowledgements

This work was supported by Texas Instruments, the NASA Center for Space Terahertz Technology and Jet Propulsion Laboratory.

References

1. W. Bishop, K. McKinney and R. Mattauch, "A Novel Whiskerless Schottky Diode for Millimeter and Submillimeter Wave Applications," *IEEE MTT-S Digest*, Vol. 2, June 1987.
2. B. Rizzi, T. Crowe and N. Erickson, "A High Power Millimeter Wave Frequency Doubler Using a Planar Diode Array," *IEEE Microwave and Guided Wave Letters*, Vol. 3, No. 6, June, 1993.
3. G. Ponchak, S. Robertson, F. Brauchler, J. East and L. Katehi, "Finite Width Coplanar Waveguide for Microwave and Millimeter Wave Integrated Circuits," to appear in *1996 International Symposium of Hybrid Microelectronics.*
4. J.East, E.Kollberg and M.Frerking, "Performance Limitations of Varactor Multipliers," *Proceeding of the Fourth International Symposiym on Space Terahertz Technology*, pp.312-325, March, 1993.

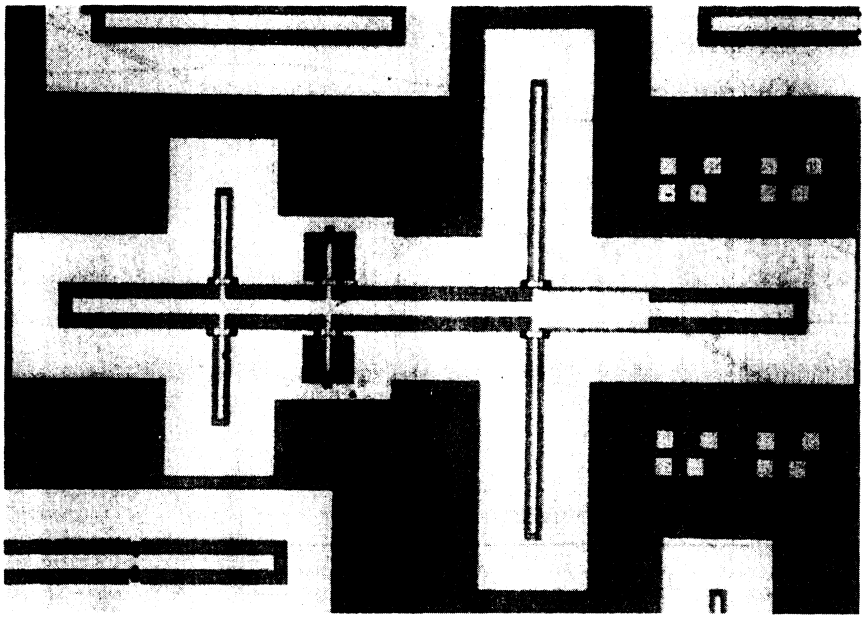

Figure 1. W-Band multiplier.

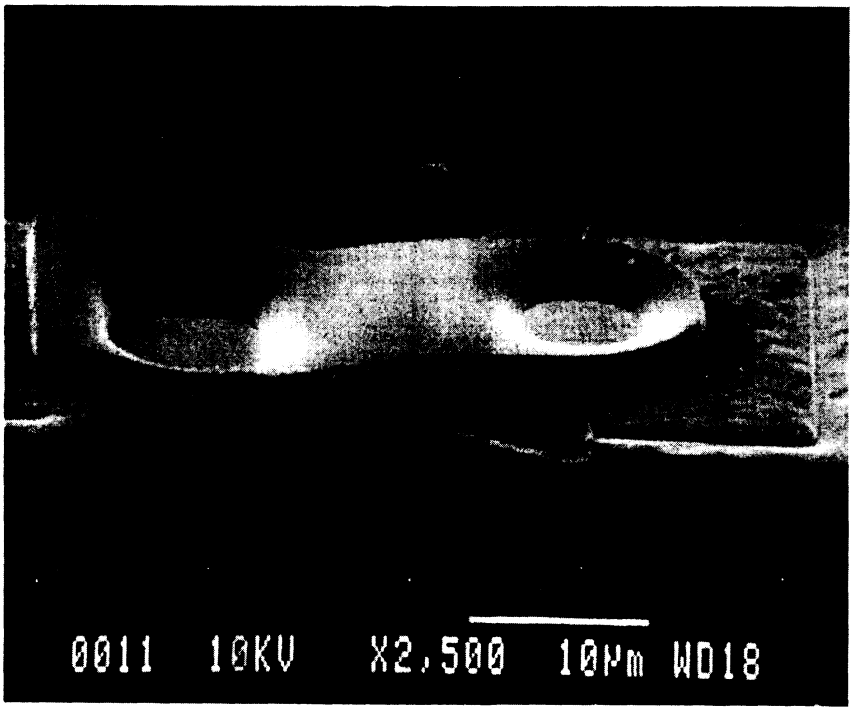

Figure 2. Diode.

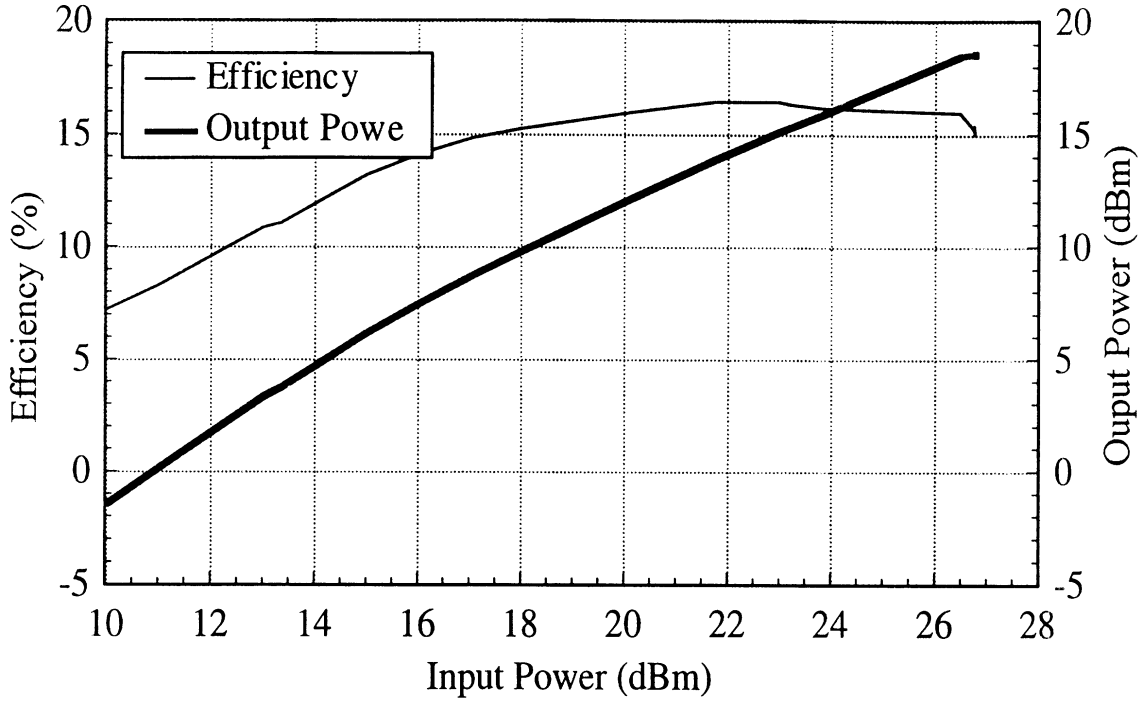

Figure 3. Measured output power and efficiency of the multiplier vs. input power.

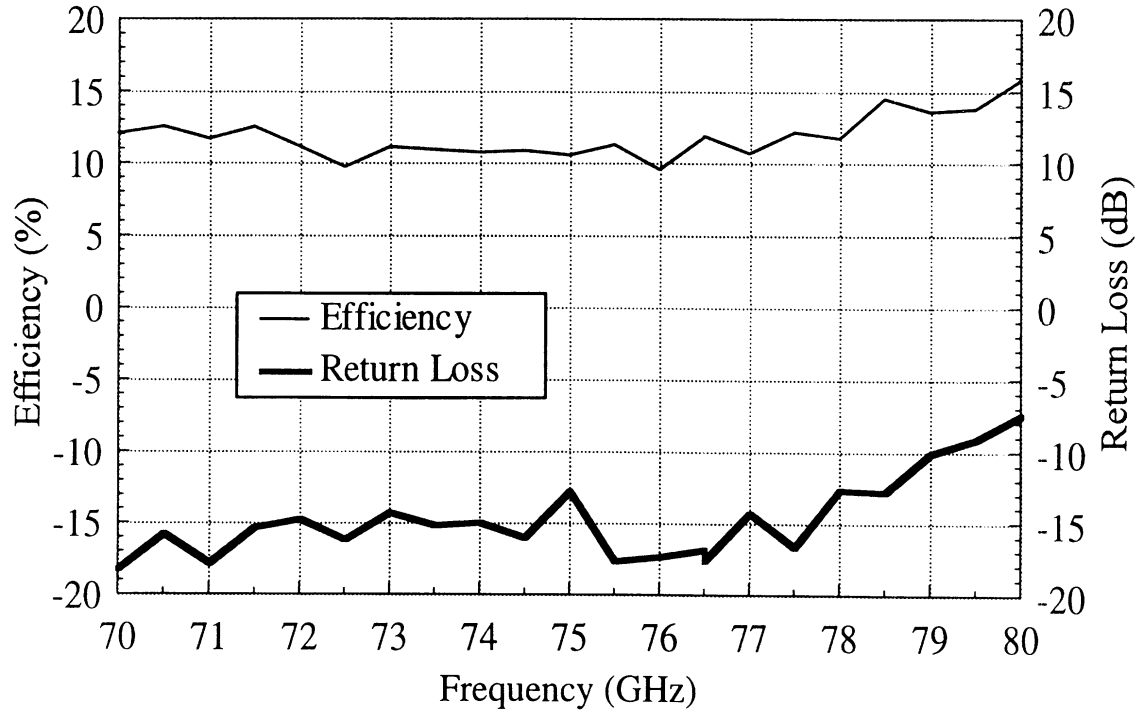

Figure 4. Measured efficiency and return loss vs. frequency.

To be presented in the 1998 IEEE International Microwave Symposium

Millimeter-Wave GaAs Monolithic Multipliers

John Papapolymerou, Jack East and Linda Katehi
EECS Department, The University of Michigan, Ann Arbor, Michigan

Moonil Kim and Imran Mehdi
Jet Propulsion Laboratory, Pasadena, California

Abstract

This paper describes the design, fabrication and experimental results for planar monolithic multipliers with output frequencies in W and D band. The multipliers are fabricated using FGC (Finite Ground Coplanar) lines which provide a low loss, low dispersion near TEM structure. This structure allows circuit fabrication on full thickness wafers with no via holes. A variety of circuits have been designed and fabricated. Different W band multipliers have an output efficiency of 22.9%, a peak output power of 66 milliwatts and an output bandwidth greater than 8 GHz in W band. Initial D band results show an uncalibrated output of approximately $100\mu W$ at 160 GHz.

I Introduction

Local oscillators are an important part of all high frequency receivers. Most high frequency multipliers use waveguide mounts. The advantages of waveguide multipliers include high Q low loss circuits, ease of tuning with E-H tuners available on both the input and output ports and a natural high pass filter configuration with cutoff waveguides. However, waveguide mount structures become smaller and more difficult to fabricate with increasing frequency. Planar monolithic multipliers provide an alternative fabrication approach that results in smaller size and volume. At the same time, they can be batch fabricated using integrated circuit techniques with lower cost than waveguide circuits. On the other hand monolithic multipliers have limitations such as higher loss and lower Q than waveguide circuits, while they lack the capability for post fabrication tuning. Conventional circuit components fabricated with microstrip lines or CPW have to be carefully designed to avoid moding at higher frequencies. A summary of some of the design tradeoffs for waveguide and monolithic multipliers along with a survey of experimental performance is given in [1]-[2].

The FGC (Finite Ground Coplanar) line is an alternative guiding structure that overcomes many of the limitations of the microstrip or CPW when operating at high frequencies. This line is similar in cross section to CPW, except that the grounds are narrow and thus prevent the parallel plate mode that can limit the high frequency operation. The resulting line supports a nearly ideal TEM propagation and can operate without backside metallization. The measured effective dielectric constant of the line is nearly constant from low frequencies up to 118 GHz and the attenuation in db/λ_g is $\propto 1/\sqrt{f}$, indicating that ohmic loss is the dominant effect. Due to the frequency dependence of ohmic losses, multipliers with FGC lines scaled at higher frequencies will experience less loss. Measured results along with more details on FGC lines that can be found in [3], show an attenuation of 0.22 dB/λ_g at 100 GHz.

II Multiplier Design

Waveguide multipliers are typically designed around an existing varactor diode. The diode capac-

itance vs. bias voltage and an estimate of the diode series resistance vs. bias and frequency are the electrical input parameters. The mounting structure must be designed around the varactor contact geometry. In contrast, in a monolithic multiplier the diode and the circuit are designed together. The first step is to choose the epitaxial layer doping that depends on the frequency and the expected electric fields which lead to possible velocity saturation in the undepleted portion of the epitaxial layer during the RF cycle. A description of velocity saturation effects is given in [4]. The design tradeoff is between a low doping to increase the breakdown voltage and the amount of power that can be absorbed before breakdown, and a higher doping to reduce the saturation effects. The wafers used in this study have an epitaxial layer doping of $10^{17}/cm^3$ and an epitaxial layer thickness of $4000\mathring{A}$. This doping level has been optimized for the W band multipliers but it was low for the D band circuits.

A nonlinear multiple reflection computer program based on [5] was written to optimize the multiplier design. The input design parameters are the epitaxial layer doping and thickness, GaAs material parameters, the desired real diode impedance and the Q at the pump frequency. The output data from this program are the embedding impedance at the second harmonic frequency, the required diode area and the estimated reverse bias voltage. The program calculates this output information for a range of input pump power levels and chooses a set of design parameters. The W band multipliers in this study have been designed with input quality factors of 2 and 3 and diode areas of 74 and 65 μm^2, respectively. The D band multipliers have a design Q of 2, and single diode areas of 40, 45 and 50 μm^2.

The next step is circuit realization using FGC lines. The dimensions of the FGC lines are limited by lithography and as a result the range of line impedances is approximately 20 to 100 Ω. Stubs are used on the input side of the circuit to trap the second harmonic output and on the output side to trap the local oscillator frequency. The diode capacitance is tuned with an inductive line connected to the circuit.

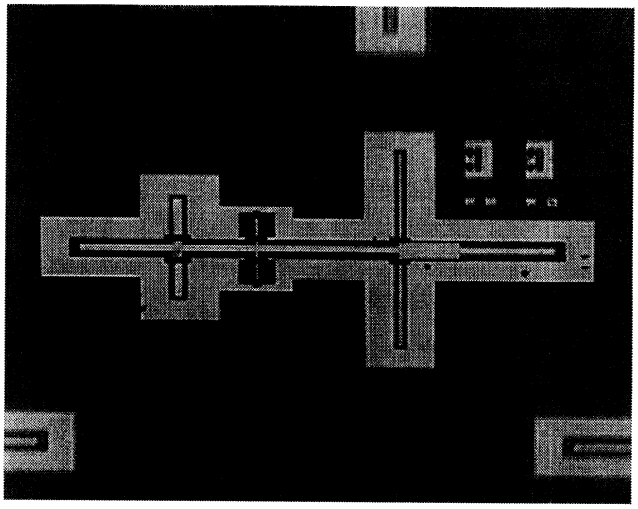

Figure 1: FGC line W-Band multiplier.

The W and D band circuits, along with calibration lines and process monitors become part of the same mask set. This mask set has been used to fabricate the experimental circuits, a sample of which can be seen in Fig. 1.

III Results and Discussion

In this section measured results from the W and D band multipliers that have been fabricated are presented.

III.1 *W-Band Multipliers*

The W band circuits have a Ka band input measurement system with a planar probe at the input and a W band probe with a waveguide section at the output. The measurements are vector error corrected to the tips of the measurement probes using a two tier error correction. A one port waveguide (Short, Offset Short, Load) calibration is used to calibrate to a waveguide flange where power can be measured with a waveguide power meter. A second one port SOL (Short Open Load) calibration is used to evaluate the waveguide to coaxial transition, a cable and the probe that form the rest of the input measurement system. The two sets of correction coefficients are combined to obtain the input port available power

and return loss. A SOL one port calibration is used to find the correction coefficients between the W band probe tip at the multiplier output and the waveguide flange location of the output power meter.

Two W band multipliers with designed Q's of 2 and 3 are evaluated. Based on simulation predictions, the low Q circuits are expected to have wider bandwidths and lower efficiencies than the higher Q versions. The high Q designs have higher peak electric fields, peak depletion layer voltages and DC reverse bias. The peak voltages in the Q=3 structures are closer to the experimental reverse breakdown voltage than the ones for Q=2. These predictions have been confirmed by the measurements. Results for the input Q = 2 circuit are shown in Figs. 2 and 3. Fig. 2 shows the power out and efficiency vs. input power for an input frequency of 38 GHz. The output power is limited by the available power of the measurement system. A peak power of 66 mW has been measured at 76 GHz. Fig. 3 shows the multiplier efficiency and return loss for a constant input drive of 20 dBm. The measurement accuracy is limited on the 80 GHz high end by the upper limit of the input Ka band system and the observed ripple is due to a standing wave in the coaxial cable between the input waveguide measurement system and the input coaxial probe. The peak efficiency is 17.6% at 76 GHz with a return loss of -5 dB and the -3 dB bandwidth is approximately 8 GHz. Results for the input Q = 3 circuit are shown in Fig. 4, where a bandwidth of approximately 6 GHz can be observed. The multiplier peak efficiency of 22.9% with a retun loss of -5 dB occurs at an input power level of 17 dBm, a much lower level than the Q = 2 circuit. The combination of a 6 GHz bandwidth with an efficiency of 22.9% makes this multiplier design unique since it offers both a very good efficiency and a broad bandwidth.

III.2 *D-Band Multipliers*

The D band circuits have a W band input probe and a D band output probe. The D band probe is a prototype and as a result the output power measurement is not calibrated since only the range of its insertion loss is known (3-6 dB). Figures 5 and 6 show the measured results for the D-Band multipliers. The input power for the frequency range of 78 to 90 GHz varies between 7.3 and 14 mW. An uncalibrated conversion loss of 20.72 dB (0.85% efficiency) is achieved at 160 GHz with the diode unbiased, and with a bias of -0.7 V an output power of $100\mu W$ is detected. Based on the minimum value of the output probe loss the output power is estimated to be $200\mu W$, while the multiplier bandwidth is measured to be 5 GHz. Other waveguide based multipliers in this frequency range have higher efficiency but are narrow band. Improvement of the D band multiplier efficiency can be achieved by appropriately optimizing the epitaxial layer profile.

The results presented herein show that scaling the FGC multiplier design to higher frequencies can still provide a reasonable efficiency while maintaining the excellent bandwidth.

IV Acknowledgments

This work was supported by the Office of Naval Research and Texas Instruments. The authors would also like to acknowledge Todd Gaier and Peter Siegel's help with the D band measurements at JPL.

References

[1] "Finite Ground Coplanar Passive and Active Circuits," Fred Brauchler, Ph.D thesis, The University of Michigan, Ann Arbor, Michigan, 1996.

[2] Fred Brauchler, John Papapolymerou, Jack East and Linda Katehi, "W Band Monolithic Multipliers," 1997 IEEE MTT-S Symposium Digest pp 1225-1228.

[3] Fred Brauchler, Steve Robertson, Jack East and Linda Katehi, "W Band Finite Ground Coplanar (FGC) Line Circuit Elements," 1996 IEEE MTT-S Symposium Digest , pp 1845-1848.

[4] J. East. E. Kollberg and M. Frerking, "Performance limitations of Varactor Multipliers," Proceedings of the Fourth International Symposium on Space Terahertz Technology, pp 312-325, March, 1993.

[5] "Microwave Mixers," S. Mass, Artech House, 1986.

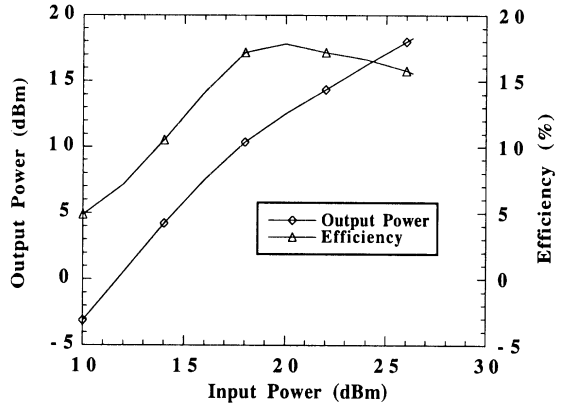

Figure 2: Efficiency and output power vs. input power at f=38 GHz for a Q=2 multiplier.

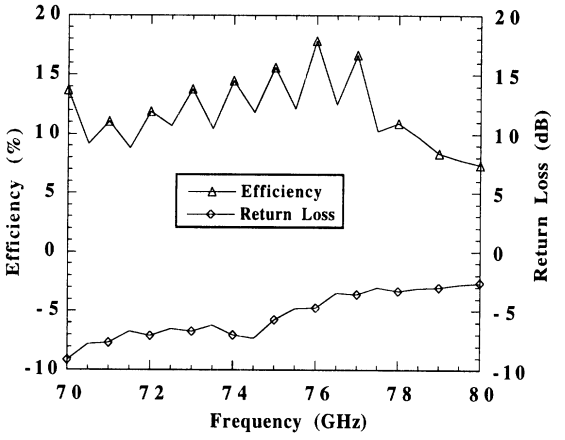

Figure 3: Efficiency and return loss vs. output frequency at P_{in}=20 dBm for a Q=2 multiplier.

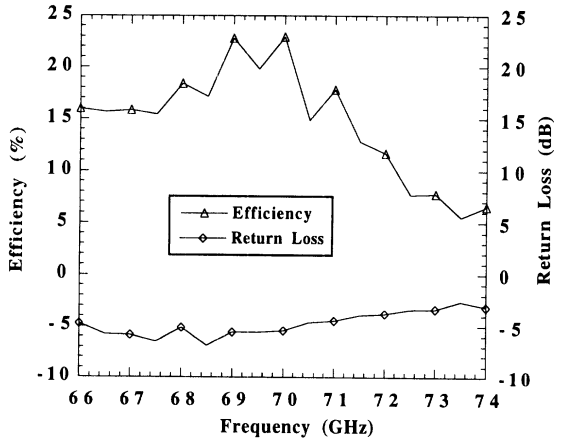

Figure 4: Efficiency and return loss vs. output frequency at P_{in}=17 dBm for a Q=3 multiplier.

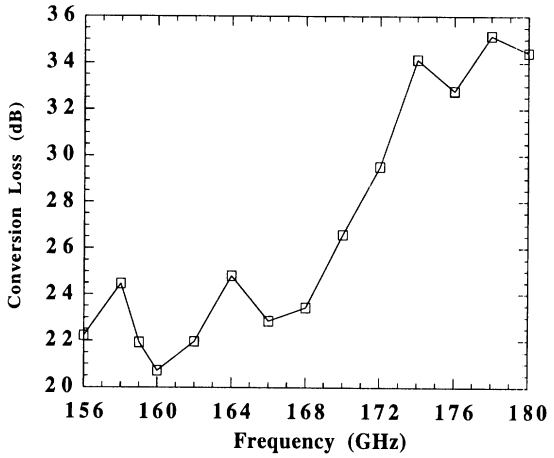

Figure 5: Conversion loss vs. output frequency for a Q=2 multiplier at zero diode bias. The results are not calibrated.

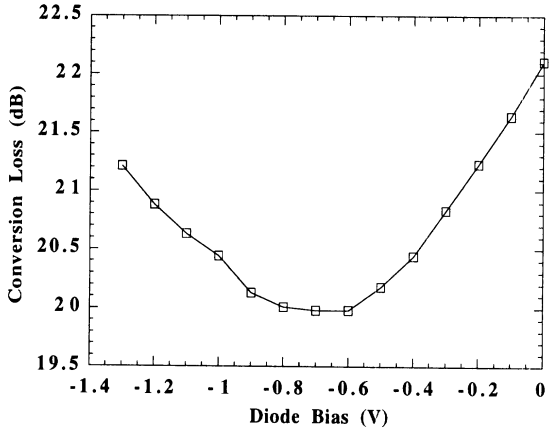

Figure 6: Conversion loss vs. diode bias at P_{in}=10 dBm and f=160 GHz for a Q=2 multiplier. The results are not calibrated.

Submitted for publication in IEEE Transactions on Microwave Theory and Techniques

GaAs vs. Quartz FGC Lines for MMIC Applications

John Papapolymerou, Jack East and Linda P.B. Katehi

Department of Electrical Engineering and Computer Science
The University of Michigan
1301 Beal Ave.
Ann Arbor, MI 48109-2122
FAX: (313) 647-2106

Abstract

The performance of FGC lines on GaAs and quartz for high frequency MMIC applications is experimentally investigated in this paper. The FGC lines on GaAs are covered with a thin layer of polyimide for passivation purposes. Permittivity and attenuation characteristics for these lines up to 118 GHz are presented and compared with the corresponding characteristics of FGC lines on a quartz substrate, commonly used for millimeter wave applications. The impact of different characteristic impedance values in attenuation properties for both GaAs and quartz is also addressed. Results indicate that the loss on the lines does not depend on the substrate material but rather on line geometry. All the lines tested show low loss and low dispersion characteristics.

1 Introduction

The Finite Ground Coplanar (FGC) transmission line is a modified Coplanar Waveguide (CPW) structure with improved performance at millimeter wave frequencies [1]. It consists of three strips, one for the signal and two for the ground, similar to the the CPW line, but with ground strips that are narrow. A back-side conductor is optional for the FGC line since the characteristics are independent of back side metallization. The main advantage of the FGC lines is that they do not support parallel-plate waveguide modes and as a result do not require via-holes for ground equalization. These vias introduce parasitics and increase fabrication complexity. The permittivity and attenuation characteristics of FGC lines on GaAs and Si have been extensively investigated by Brauchler [2]. Experimental results show that a nearly TEM mode propagates over a wide frequency range (2-118 GHz) and that loss is mainly ohmic. The use of full thickness substrates and the elimination of via holes for mode suppression will reduce the cost and complexity of MMIC design and fabrication at millimeter wave frequencies. The purpose of this short paper is to discuss the effect of polyimide passivation on these lines and to compare lines with different dimensions on both GaAs and quartz substrates. The results confirm the excellent performance of the FGC lines on GaAs.

High performance line structures are an important part of MMIC design and fabrication at millimeter wave frequencies [3]. Conventional microstrip lines have increasing dielectric loss with frequency. One solution to this problem is to use a low loss material such as quartz as a substrate. However, this requires bonding active circuits onto the quartz, which increases fabrication complexity especially at higher frequencies, while at the same time the requirement for thinned substrates for microstrip or via holes for CPW is still important to satisfy. FGC lines are conductor loss dominated, so the use of semiconductor substrates will have a small effect on the line loss properties. Furthemore, passivation is also an important part of MMIC fabrication. Polyimide is a well characterized dielectric material that has been extensively used in the past as a passivation layer and as a substrate for the fabrication of microstrip lines [4]-[5]. In this paper we investigate the effect of a thin polyimide coating on top of the GaAs FGC lines and compare their performance with low loss quartz based lines. The cross section of the fabricated FGC lines can be seen in Fig.1. Four configurations have been fabricated and tested: a) FGC lines on GaAs with Z_o=40, 50 and 60 Ω, b) FGC lines on GaAs with a 2 μm thick polyimide overlay and $Z_o = 50\ \Omega$, c) FGC lines on

GaAs with a 3 μm thick polyimide overlay and $Z_o = 50\ \Omega$ and d) FGC lines on quartz with Z_o=70, 90 and 100 Ω.

2 Fabrication

FGC lines have been fabricated on a 525 μm thick semi-insulating GaAs wafer and a 165 μm thick quartz wafer. The FGC line signal-strip (w), slot (s) and ground-strip (w_g) widths are 50, 45, 160 μm, respectively and correspond to a 50 Ω line for GaAs substrate and to 90 Ω for quartz substrate. The lines have been created by using standard lift-off process with a total metal thickness of 1 μm. After the lines are formed, polyimide Pyralin PI2545 is spun at 4 Krpm and 2.5 Krpm on top of the lines for two GaAs wafers, in order to get a thickness of 2 μm and 3 μm respectively. The pre-cure temperature for the polyimide film is 140^o C and the hard-cure 200^o C while the baking time is set to 30 minutes and 3 hours respectively. At the beginning and the end of the FGC lines the polyimide is chemically etched in order to allow the probe tips of the measurement system to be in electrical contact with the lines. The relative dielectric constant of the polyimide film is 3.5. The test FGC lines consisted of a thru line with a length of 1.0 mm, a short with a length of 0.5 mm and 3 delay lines with 1.388 mm, 4.106 mm and 10 mm lengths respectively.

3 Results and Discussion

All of the mesurements for the FGC line characteristics have been performed with an HP8510 network analyzer and a probe station using a variety of RF probes. De-embeding is achieved by performing a Thru-Reflect-Line (TRL) calibration with the help of Multical [6], a measurement program available from NIST. This program also provides the effective dielectric permitivity and attenuation characteristics of the lines under test, from the delay line measurements.

The effective dielectric constant of the various line configurations is shown in Fig. 2. As can be seen, the nearly constant behavior of ϵ_{eff} over the entire frequency range indicates the propagation of a nearly pure TEM mode. In addition, we observe that the thin film of polyimide is responsible for a slight increase in ϵ_{eff} for both the 2μm polyimide (1.4%) and the 3μm polyimide (2.8%) when compared to that of bare FGC lines. This increase is more pronounced at higher frequencies. However, ϵ_{eff} is comparable with that of bare lines over the entire frequency range , indicating

that the addition of polyimide does not significantly change the propagation characteristics of the lines.

Fig. 3 shows the attenuation per physical length for the four different cases. The straight line between 60 and 70 GHz represents a gap in the data. As can be seen, the polyimide increases the attenuattion constant with the effect being more pronounced in W-band (12%) and for the thicker polyimide (23% in W-band). The quartz has the smallest attenuation for all the lines. This lower loss when measured in dB/cm is due to the lower effective dielectric constant and higher characteristic impedance of the FGC line on quartz (90 Ω compared to 50 Ω for GaAs). Since in most microwave circuits lengths are expressed in terms of wavelengths, the attenuation per guided wavelength for the four different lines has been evaluated and is shown in Fig. 4. The results are comparable for all four cases with GaAs (bare or with polyimide) being slightly better than quartz. This indicates that the loss of FGC lines is ohmic in nature and independent of the substrate material. As a result, FGC lines are very good candidates for high frequency application circuits. Furthemore, we can conclude that the thin layer of polyimide that covers the FGC lines on GaAs for passivation purposes does not increase the total loss of the lines.

Since the characteristic impedances for the lines investigated were different for GaAs and quartz, additional lines with varying dimensions and impedances have been fabricated. The impedance range for the two substrates corresponds to a convenient range for line fabrication. The line dimensions and the corresponding Z_o can be seen in Table 1. From the measured attenuation per physical length, the attenuation per guided wavelength has been evaluated and can be seen in Fig.5 for GaAs and Fig.6 for quartz. From Fig. 5 we observe that the 50 and 60 Ω lines have practically the same attenuation while for the 40 Ω line there is an increase of about 100% at 60 GHz which is the center of the entire frequency range. Similarly, from Fig. 6 we observe that the attenuation for the 90 and 100 Ω lines is almost the same and that the 70 Ω line exhibits a 60% increase from the other two lines at 60 GHz. We should note here that the small ripple observed in the 90 and 100 Ω lines is due to ripple in the mismatched measurement system.

In order to better understand the behavior of the FGC lines versus impedance, the measured attenuation per physical length data have been curve fitted to a $a+b\sqrt{f}$ function and the extracted functions have been used in order to evaluate the attenuation per guided wavelength for three different frequency points in the center of each measured band. The final results can be seen in

Table 1: Geometrical characteristics for fabricated lines

substrate	w (μm)	s (μm)	Z_o (Ω)
GaAs	50	15.45	40
GaAs	50	64.5	60
Quartz	50	18.61	70
Quartz	50	64.5	100

Figs. 7-9 for both quartz and GaAs. From these figures we observe that the attenuation decreases as the impedance increases in a non-linear way. In terms of loss in dB/λ_g a 50 or 60 Ω line on GaAs is equivalent to a 90 Ω line on quartz. However, we should note that the 50 Ω and 60 Ω GaAs lines have the same geometrical dimensions with the 90 Ω and 100 Ω lines on quartz respectively, indicating a strong dependence of the total line loss on the geometrical characteristics rather than the substrate material and thickness. This feature makes FGC lines ideal for high frequency MMIC's.

Having found that in terms of loss GaAs and quartz are equivalent for the same FGC geometry, the choice of material for a substrate depends on other design criteria. If low cost is a major issue then quartz can be chosen with the active devices being flip-chip bonded to it. On the other hand if the active devices must be monolithically integrated with the rest of the circuitry, then GaAs is more appropriate with a thin overlay of polyimide for passivation. GaAs is also more suitable for applications above 120 GHz where the flip-chip bonding process increases fabrication complexity considerably.

4 Conclusions

FGC lines on GaAs with a thin overlay of polyimide have been fabricated and tested. Experimental results show a negligible increase in the effective dielectric constant and a small increase in the attenuation per physical length, when compared with bare FGC lines on GaAs. The attenuation per physical length of FGC lines on GaAs with or without polyimide is higher than that of FGC lines on quartz. The attenuation per guided wavelength, however, is almost the same for all types of

lines investigated in this paper, indicating that the total loss of FGC lines with the same geometry is independent of the substrate material. This allows for the use of a thin layer of polyimide over FGC lines on GaAs without increasing the total loss in actual circuits while providing passivation at the same time. In addition, the attenuation of the lines decreases in a non linear fashion versus characteristic impedance. Finally, FGC lines with a polyimide overlay can be used in millimeter wave receivers and transmitters fabricated on GaAs, where the active devices are monolithically integrated with the other circuitry and do not need to be flip-chip bonded as in the case of quartz.

5 Acknowledgement

The authors would like to acknowledge the help of Dr. Imran Mehdi of the Jet Propulsion Laboratory for providing the quartz material used in these experiments. This work has been partially supported by the Office of Naval Research and partially by NASA/JPL.

References

[1] F. Brauchler, S. Robertson, J. East and L.P.B Katehi, "W-Band Finite Ground Coplanar (FGC) Line Circuit Elements," *IEEE MTT-S International Symposium Digest,* June 1996.

[2] F. Brauchler, "Finite Ground Coplanar Passive and Active Circuits," *Ph.D. Dissertation,* The University of Michigan, Ann Arbor, 1996.

[3] F. Brauchler, J. Papapolymerou, J. East and L.P.B. Katehi,"W-Band Monolithic Multipliers,"*IEEE MTT-S International Symposium Digest,* June 1997.

[4] G. Ponchak, A. Downey and L.P.B. Katehi, "High Frequency Interconnects on Silicon Substrates," *Radio Frequency Integrated Circuit (RFIC) Symposium,* June 1997.

[5] H. Ogawa, T. Hasegawa, S. Banba and H. Nakamoto,"MMIC Transmission Lines for Multi-Layered MMIC's," *IEEE MTT-S International Symposium Digest,* June 1991.

[6] R.B. Marks and D.F. Williams,"Program MultiCal," *rev. 1.00, NIST,* August 1995.

Figure Captions

Fig.1 FGC lines on GaAs with a polyimide overlay.

Fig.2 Effective dielectric constant vs. frequency for the various FGC lines.

Fig.3 Attenuation per physical length vs. frequency for the various FGC lines.

Fig.4 Attenuation per guided wavelength vs. frequency for the various FGC lines.

Fig.5 Attenuation per guided wavelength for lines on GaAs with different Z_o.

Fig.6 Attenuation per guided wavelength for lines on quartz with different Z_o.

Fig.7 Attenuation per guided wavelength vs. characteristic impedance for lines on GaAs and quartz at f=19.1 GHz.

Fig.8 Attenuation per guided wavelength vs. characteristic impedance for lines on GaAs and quartz at f=50 GHz.

Fig.9 Attenuation per guided wavelength vs. characteristic impedance for lines on GaAs and quartz at f=94 GHz.

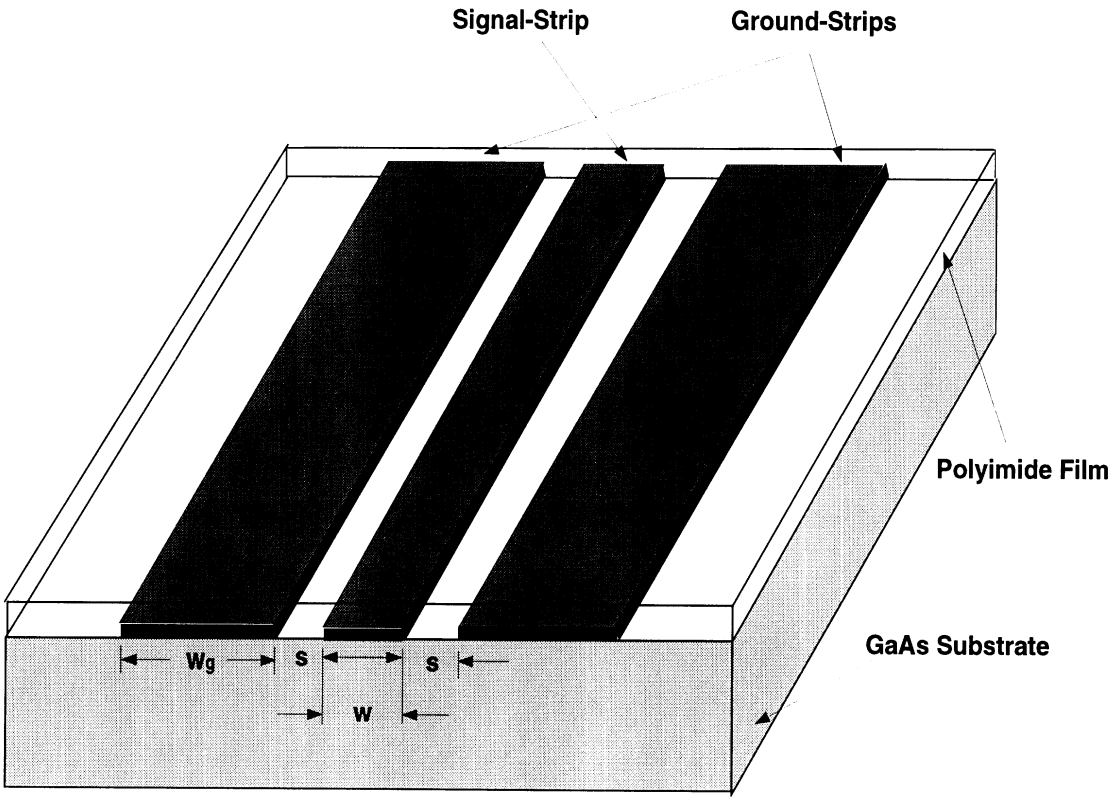

Figure 1: FGC lines on GaAs with a polyimide overlay.

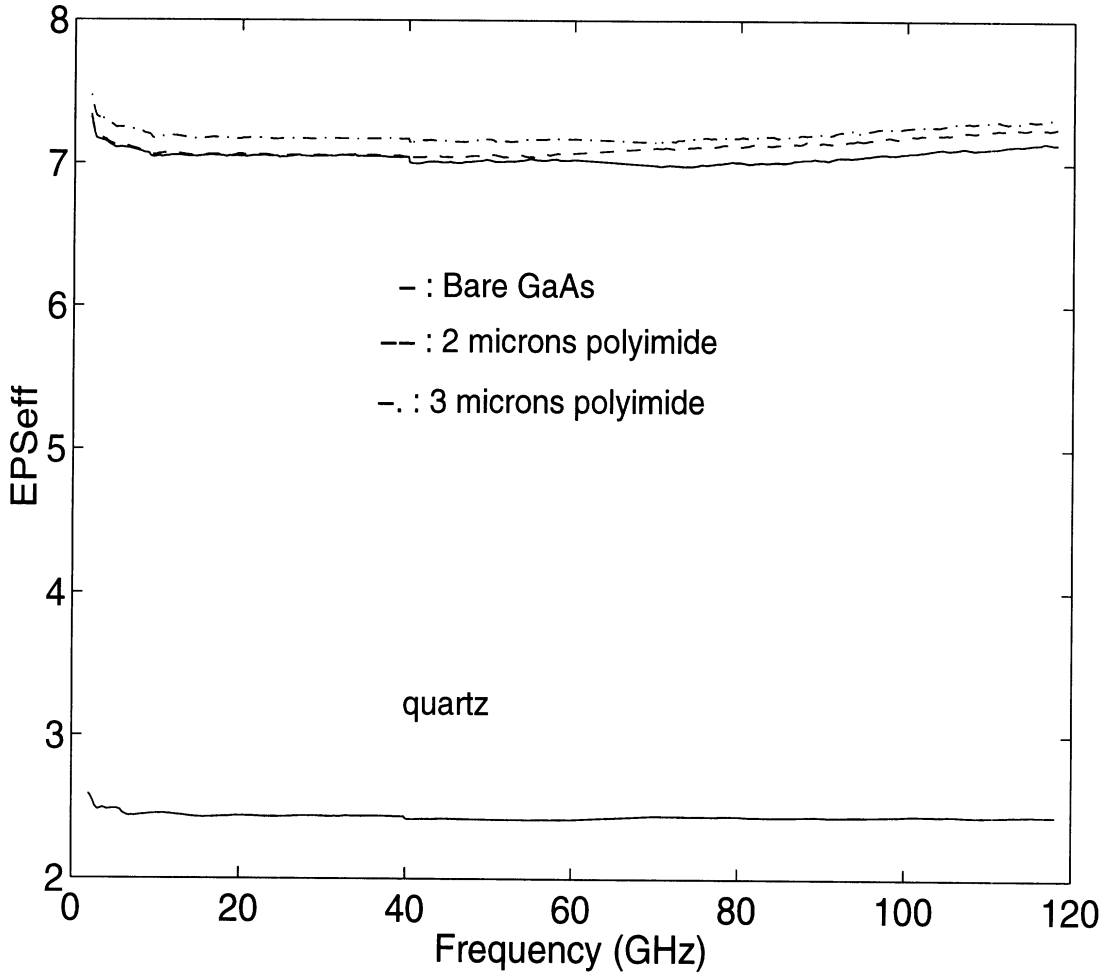

Figure 2: Effective dielectric constant vs. frequency for the various FGC lines

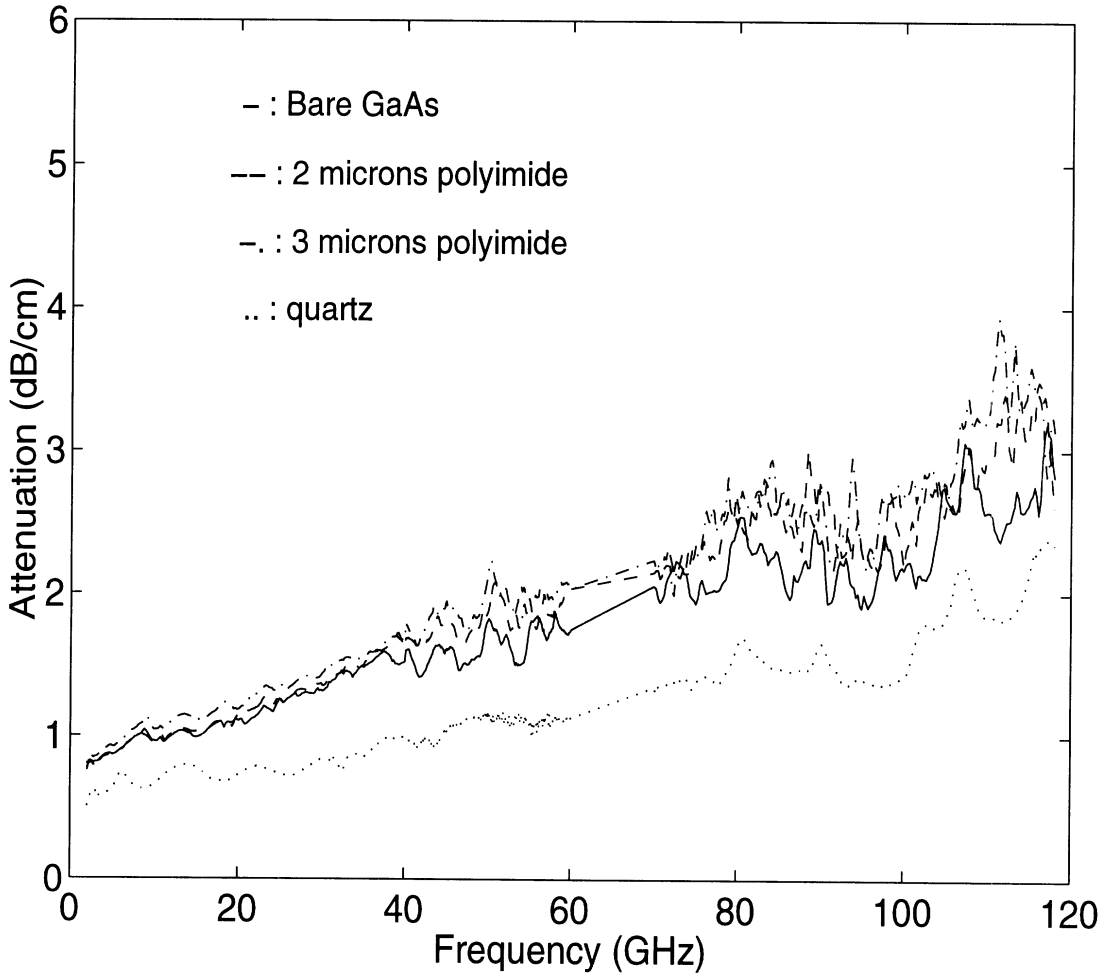

Figure 3: Attenuation per physical length vs. frequency for the various FGC lines

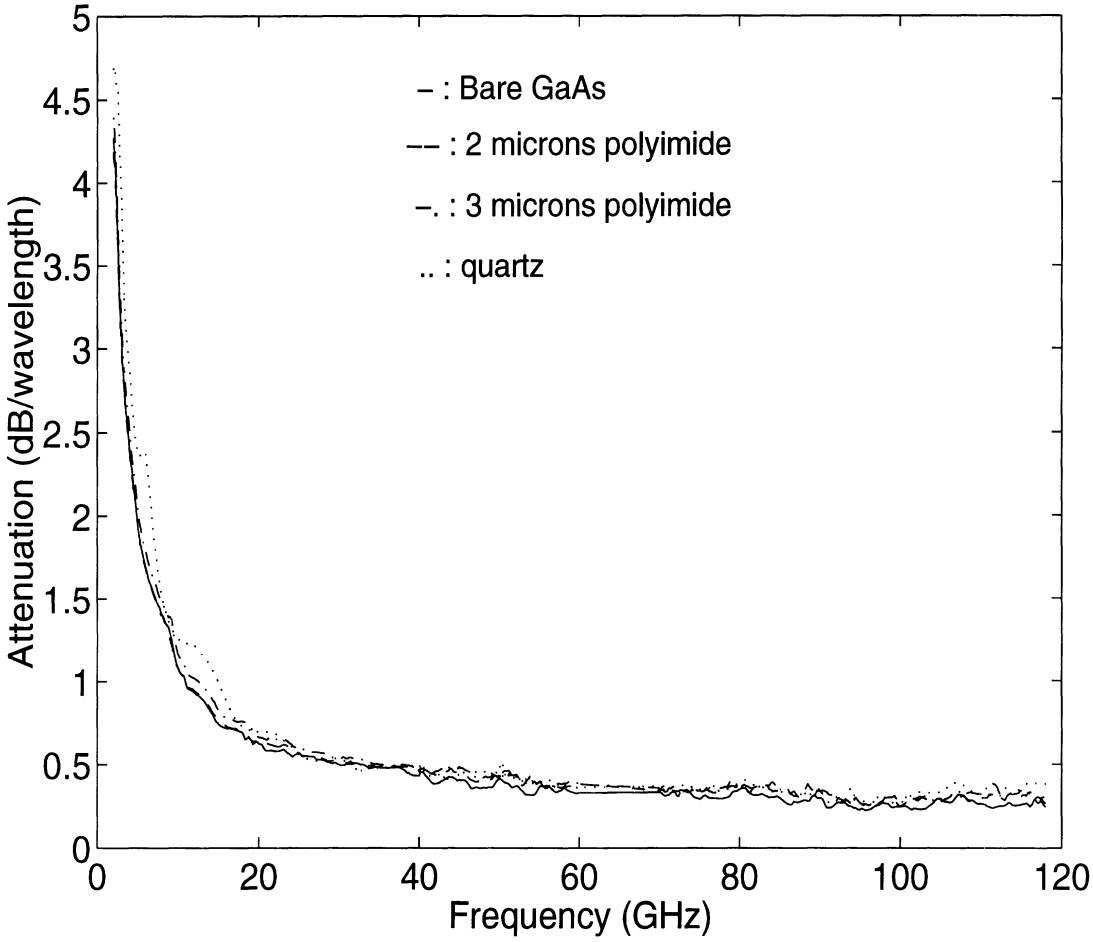

Figure 4: Attenuation per guided wavelength vs. frequency for the various FGC lines

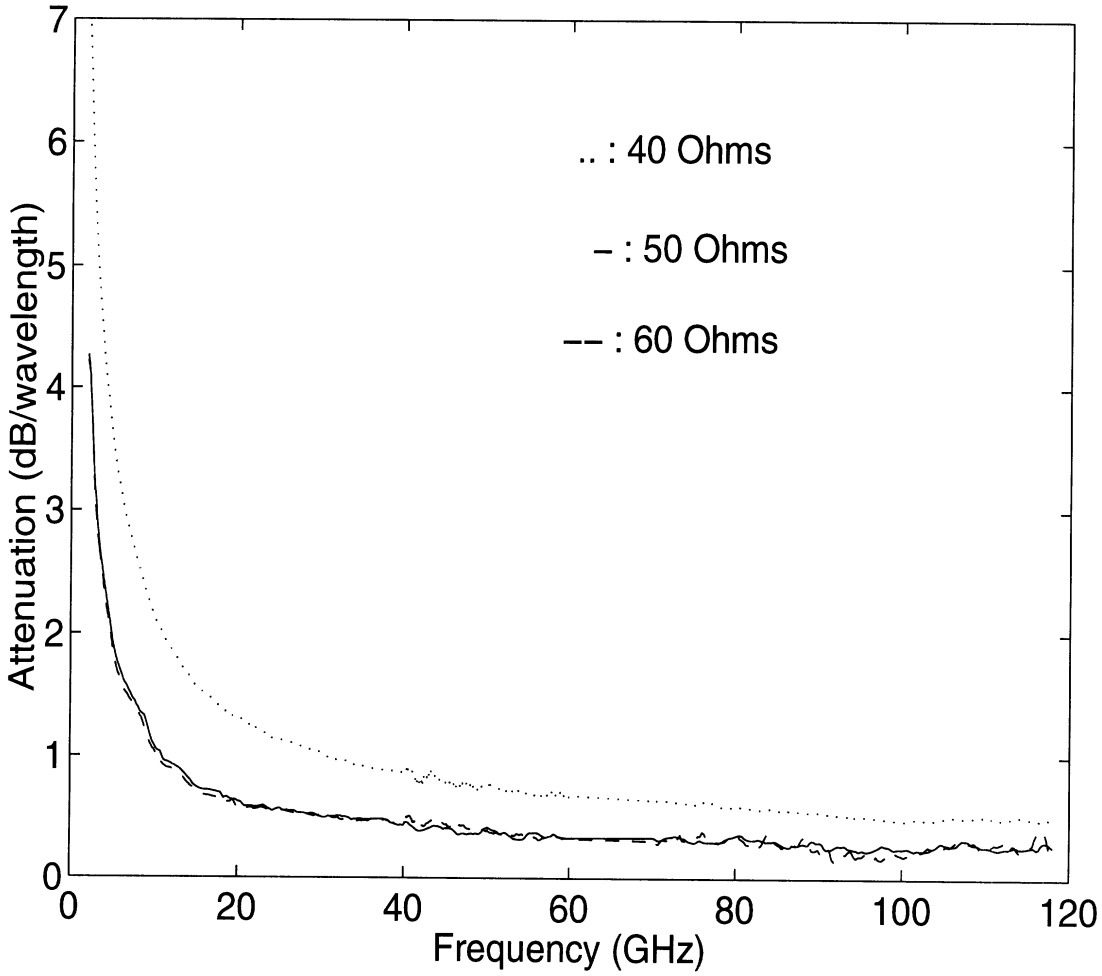

Figure 5: Attenuation per guided wavelength for lines on GaAs with different Z_o

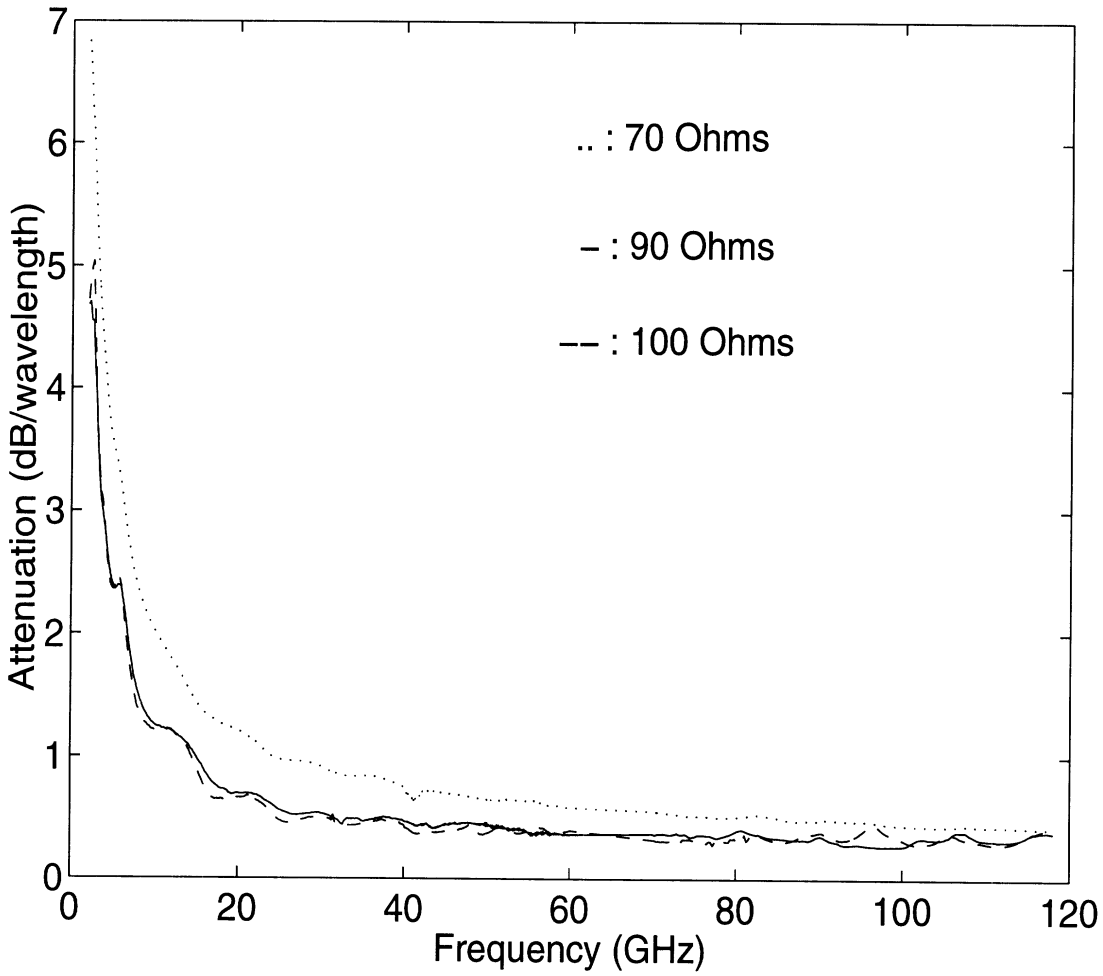

Figure 6: Attenuation per guided wavelength for lines on quartz with different Z_o

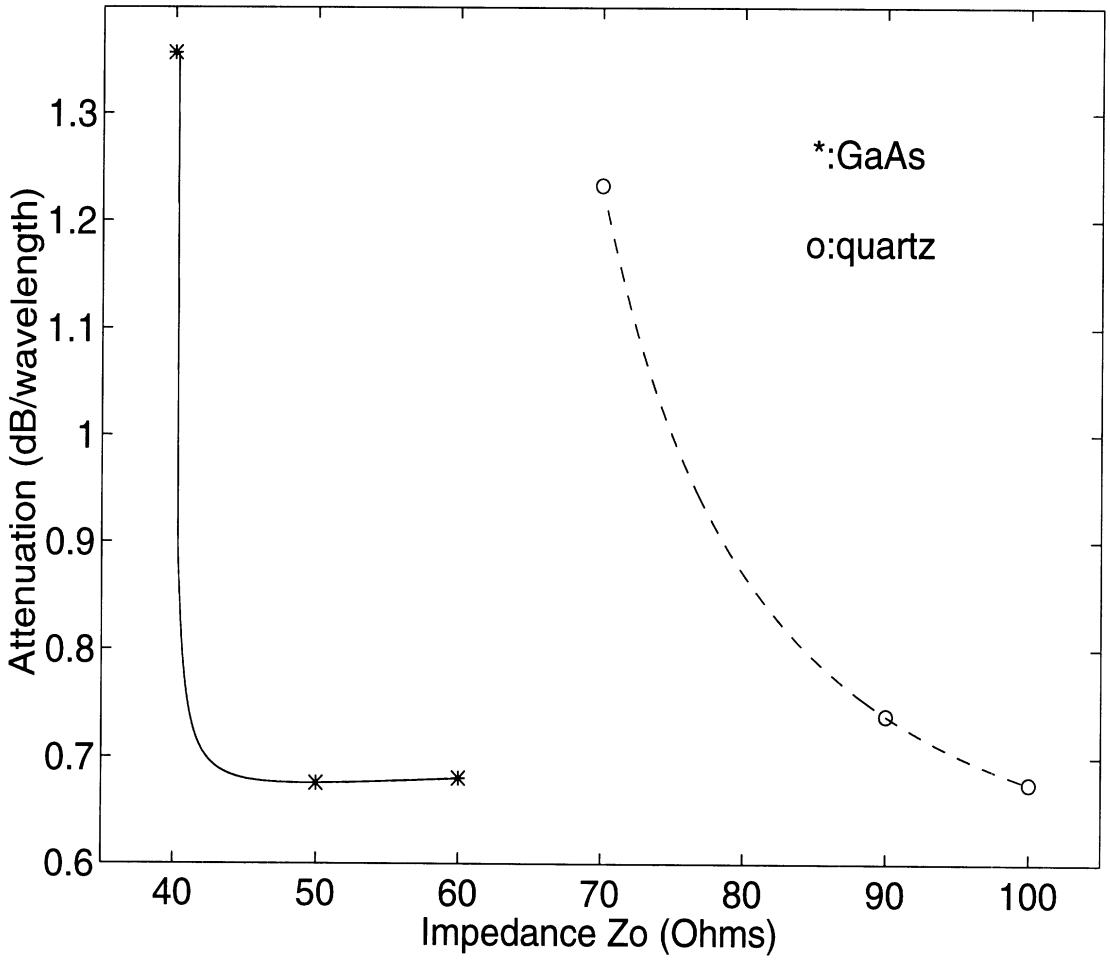

Figure 7: Attenuation per guided wavelength vs. characteristic impedance for lines on GaAs and quartz at f=19.1 GHz

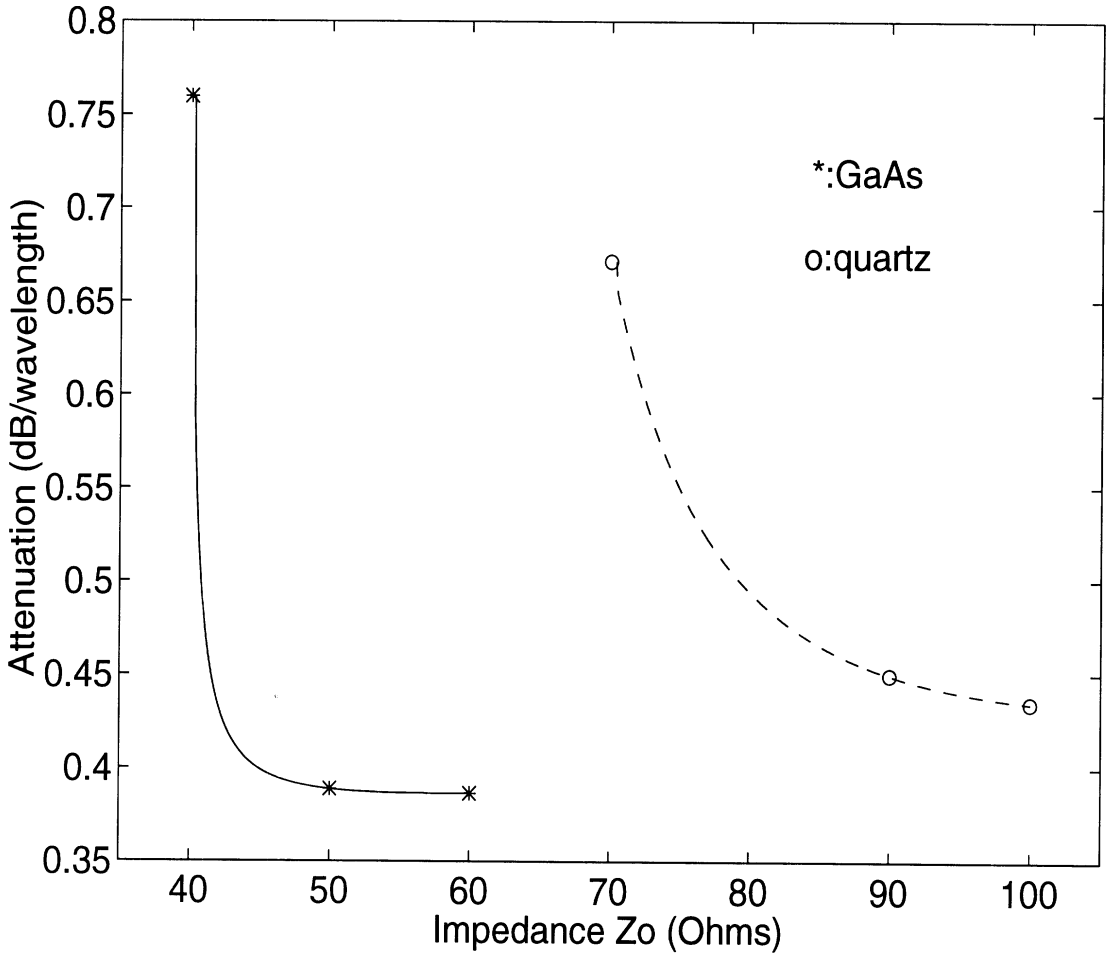

Figure 8: Attenuation per guided wavelength vs. characteristic impedance for lines on GaAs and quartz at f=50 GHz

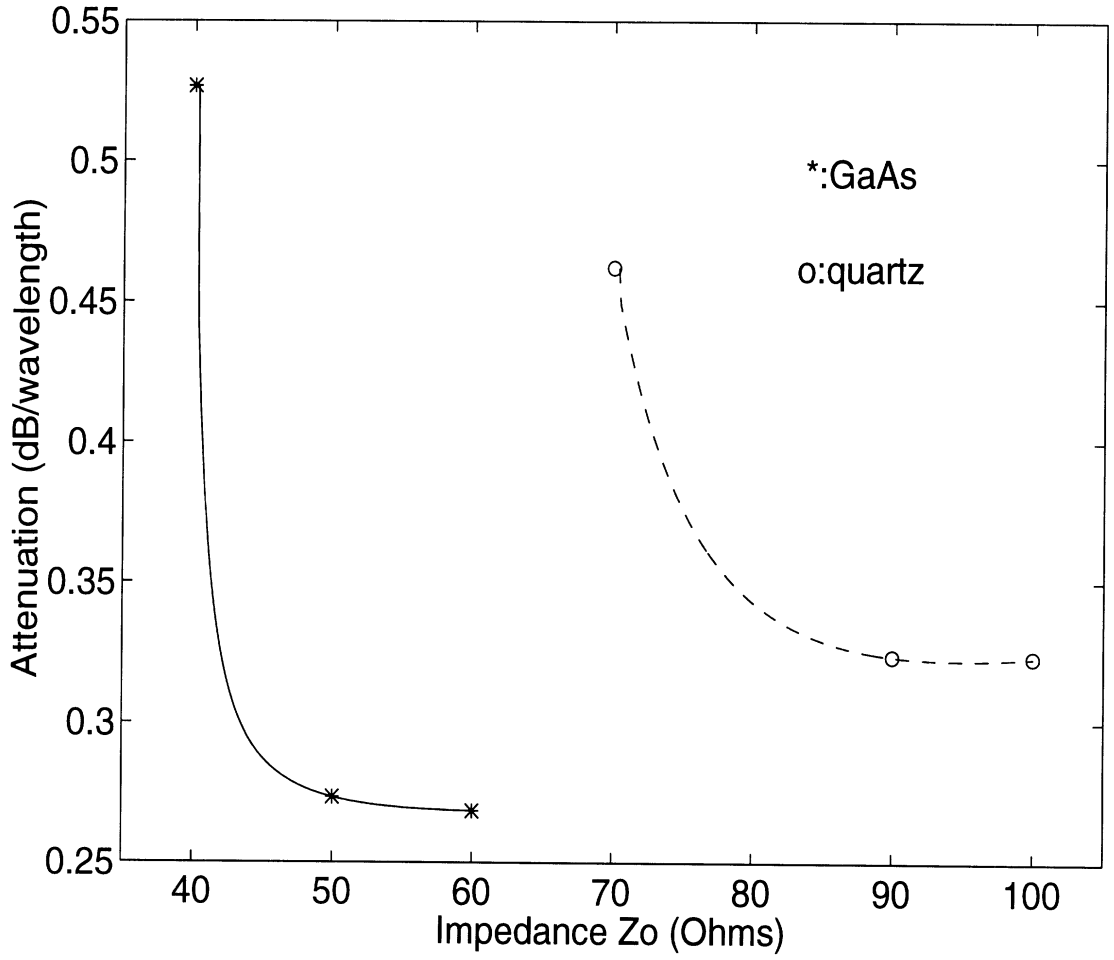

Figure 9: Attenuation per guided wavelength vs. characteristic impedance for lines on GaAs and quartz at f=94 GHz

Submitted to IEEE AP-S 1998 Int'l Symposium (Jan. 12, 1998)

Suppression of Surface Waves Using the Micromachining Technique

Jong-Gwan Yook* and Linda P. B. Katehi
Radiation Laboratory
Department of Electrical Engineering and Computer Science
The University of Michigan, Ann Arbor, MI 48109-2122, U. S. A.
Tel: 313-764-0608, Fax: 313-647-2106, Email: yookjong@engin.umich.edu

ABSTRACT

In this paper, silicon micromachining has been applied to build high performance microwave and millimeter-wave antennas. To suppress substrate modes and increase the bandwidth of the patch antenna, silicon substrate material has been selectively removed under the patch area. It has been shown in this paper that the new structure can effectively suppress unwanted substrate and higher order modes. Also, effective dielectric constant curves for micromachined substrates are provided for accurate design of patch antennas.

I. INTRODUCTION

With the advance of MMIC and silicon technologies, microwave and Millimeter-wave circuits and antennas are integrated into smaller areas on high index materals, such as silicon. Silicon substrate has special advantages in MMICs and antenna applications due to its compatibility with active and passive circuits. Furthermore, recent development of silicon micromaching technology[1]–[4] offers another possibility of efficient microstrip patch antenna.

High index substrate material (ex. $\epsilon_r = 11.7$) allows smaller overall circuit and antenna size. However, onset of substrate modes result in low radiation efficiency, thus limiting the performance of patch antennas on these materials. To overcome these difficulties, selective removal of substrate material has been proposed recently[5, 6]. It has been shown that the silicon micromachined microstrip patch antenna exhibits better radiation efficiency than conventional antenna.

In this paper, we take a close look at what causes that kind of phenomenon and how we can accurately design patch antennas on silicon micromachined substrates. For theoretical modeling, a multilayer method of moment technique and a 3-dimensional finite element method have been employed.

II. THEORETICAL MODELING

For modeling of micromachined antenna components, full-wave techniques, such as a multilayer method of moment(MoM)[7, 8] and finite element method(FEM)[9] have been applied. Specifically, the finite element method has been parallelized on a distributed memory parallel computer for maximum efficiency using the message passing interface (MPI). MPI allows us inter-platform portability between various parallel computer architectures. To handle open boundary problems, artificial absorbing material has been adapted in the FEM.

III. MICROMACHINED ANTENNAS

A. Effective Dielectric Constant

To accurately predict the effective dielectric constant of the micromachined material, the MoM techniques are applied to find resonant frequency of the patch antenna printed on micromachined material as shown in Fig.1. The effective dielectric constant is defined as

$$\epsilon_{r.eff} = (\frac{c}{2Lf_r})^2 \tag{1}$$

where c, L, and f_r are the speed of light, patch resonant length, and resonant frequency, respectively. As can be observed from the plots, the effective dielectric constant is a function of patch length (L) as well as silicon-to-air ratio. It is interesting to note that the $\epsilon_{r.eff}$ for a large patch on 100 % silicon or air substrate are not 12 or 1 in each case. For transmission lines on this type of layered substrate, one can obtain accurate dielectric constant values in a limited range using formula in [10].

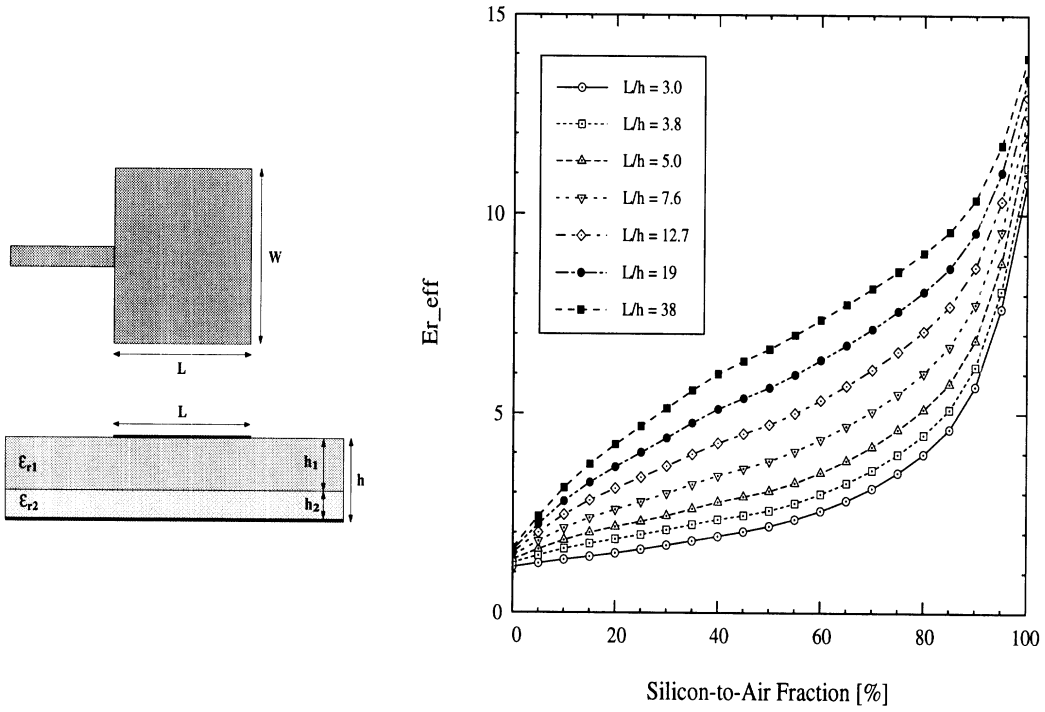

Figure 1: (a) Microstrip patch antenna on double layer substrates: $\epsilon_{r1} = 12.0$ (silicon), $\epsilon_{r2} = 1.0$ (air). (b) Effective dielectric constant curves for micromachined antenna: L = patch resonant length, $\mathbf{h}$ = substrate thickness ($\mathbf{h_1} + \mathbf{h_2}$), and silicon-to-air fraction = $(\mathbf{h_1}/\mathbf{h}) \times 100$ [%].

B. Microstrip-Fed Slot-Coupled Micromachined Patch Antenna

To examine the electromagnetic field distribution in the micromachined antenna structure, the microstrip-fed slot-coupled micromachined patch antennas[6] have been analysed using the 3D parallel FEM. As shown in Fig.2 (a) and (b), full substrate and micromachined substrate (75 % etched) are used and the electric field components, tangential and normal to the surface, and total, are examined as dipicted in Fig.3. As it can be observed, removal of the substrate material under the patch element increases the field confinement in the undelying cavity in two different cases (2h and 4h cases) and thus allows reduced substrate mode. In particular, the normal electric field components are very well concentrated only under the patch and eventually reduce the interactions between the radiating element in a large array configuration.

As an application of the micromachined patch antenna, a W-band antenna has been designed with H-shape slot and 75 % silicon removal. The return loss and radiation loss are computed using the FEM. The bandwidth of the antenna is larger than 12 % and radiaiton loss ls computed as $10log(1 - |S_{11}|^2)$.

IV. Conclusions

In this paper, silicon micromachined structures have been presented as a new efficient microstrip patch antenna. It is shown that the micromachined substrate can effectively suppress the surface wave excitation and thus increase antenna efficiency. The field confinement under the patch can be applied to build ideal array antennas having good isolation between the radiating elements.

Acknowledgment

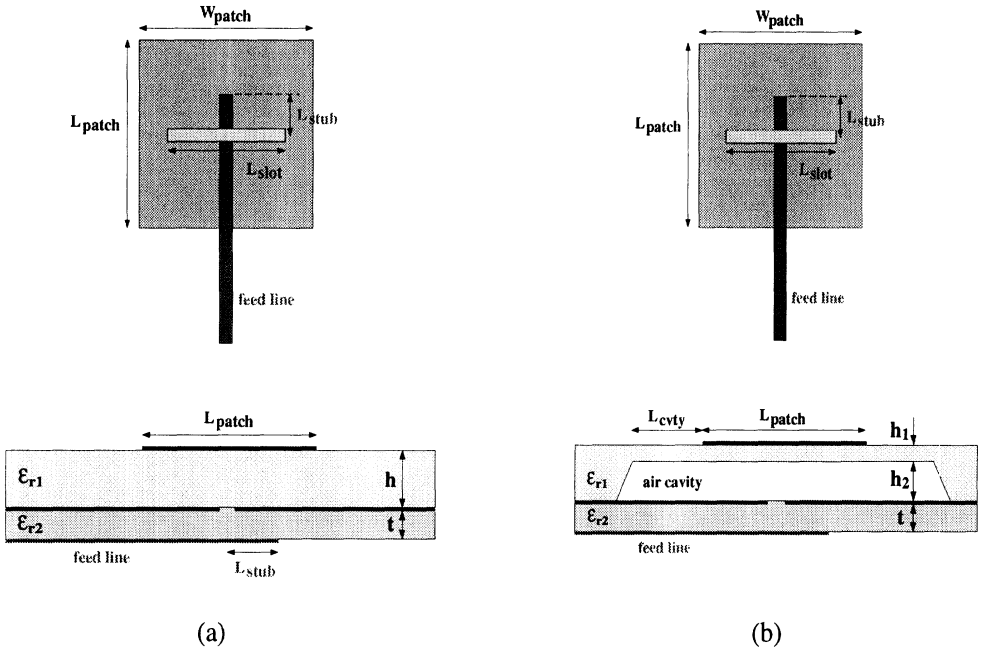

(a) (b)

Figure 2: Microstrip-fed slot-coupled patch antennas: (a) on full substrate (0% etched), (b) on micromachined substrates (75% etched).

This work was partially supported by Hughes/DARPA. Also, the authors would like to thank the University of Michigan Center for Parallel Computing (CPC), which is partially funded by NSF grant CDA-92-14296 and the Ford Motor Company, for the use of computational facilities.

References

[1] T. Weller, L. Katehi, G. Rebeiz, "High performance microshield line components", *IEEE Transactions on Microwave Theory and Techniques*, Vol. 43, pp. 534–543, Mar. 1995.

[2] S. Robertson, L. Katehi, G. Rebeiz, "Micromachined W-band filters", *IEEE Transactions on Microwave Theory and Techniques*, Vol. 44, pp. 598–606, Apr. 1996.

[3] R. Drayton, L. Katehi, "Development of self-packaged high frequency circuits using micromachining techniques",*IEEE Transactions on Microwave Theory and Techniques*, Vol. 43, pt.1, pp. 2073–2080, Sep. 1995.

[4] V. Milanovic, M. Gaitan, E. Bowen, "Micromachined microwave transmission lines in CMOS technology", *IEEE Transactions on Microwave Theory and Techniques*, Vol. 45, pt.1, pp. 630–635, May 1997.

[5] I. Papapolymerou, R. Drayton, L. Katehi, "Micromachined Patch Antenna," *IEEE Transactions on Antennas and Propagations*, Feb. 1998(to be appear).

[6] G. Gauthier, L. Katehi, and G. Rebeiz, "A 94 GHz Aperture-Coupled Micromachined Microstrip Antenna," *1998 IEEE MTT-S Int'l Symposium*(submitted).

[7] HP EEsof, Inc: Westlake Village, CA.

[8] IE3D, Zeland Software, Inc: Fremont, CA.

[9] J.-G. Yook, N. Dib and L. Katehi, "Characterization of High Frequency Interconnects Using Finite Difference Time Domain and Finite Element Methods", *IEEE Transactions on Microwave Theory and Techniques*, Vol. 42, pp. 1727–1736, Sep. 1994.

[10] P. Pramanick and P. Bhartia, "Computer-Aided Design Models for MIllimeter-Wave Finlines and Suspended-Substrate Microstrip Lines," *IEEE Transactions on Microwave Theory and Techniques*, Vol. 33, pp. 1429–1435, Dec. 1985.

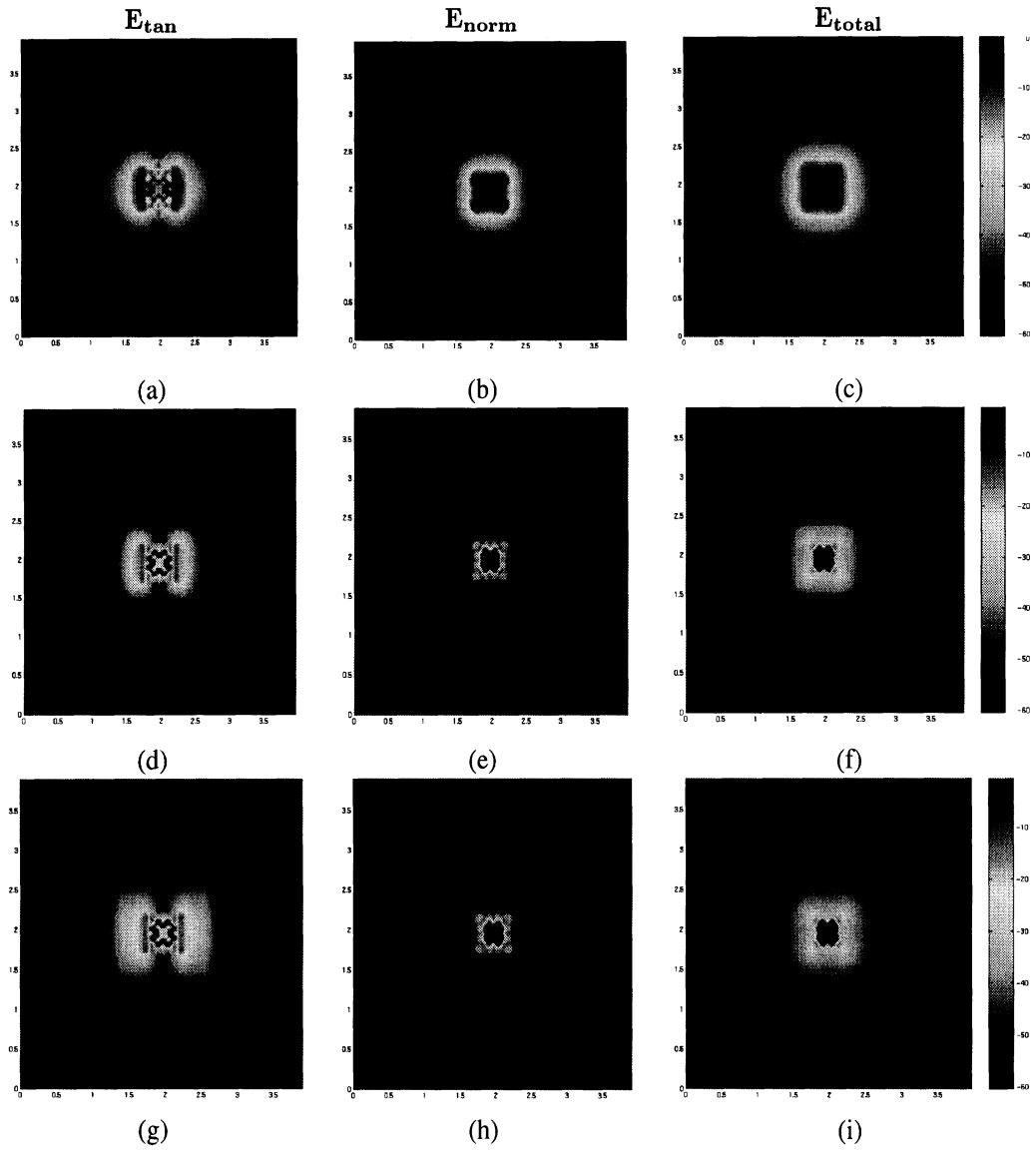

Figure 3: Electric field distributions at 90 GHz. (a), (b), (c): Conventional microstrip patch antenna, (d), (e), (f): micromachined (75% Si removed at L_{cvty} = 2h distance) patch antenna, (g), (h), (i): micromachined (75% Si removed at L_{cvty} = 4h distance) patch antenna.